Photochromic Formazans: Raman Spectra, *X*-Ray Crystal Structures,† and ^{13}C Magnetic Resonance Spectra of the Orange and Red Isomers of 3-Ethyl-1,5-diphenylformazan

Gary R. Burns * **and Christopher W. Cunningham**
Chemistry Department, Victoria University, Private Bag, Wellington, New Zealand
Vickie McKee
Chemistry Department, University of Canterbury, Christchurch 1, New Zealand

The *X*-ray crystal structures of the two isomers of a photochromic formazan have been determined. Red 3-ethyl-1,5-diphenylformazan belongs to the orthorhombic space group $P2_12_12_1$ and adopts a *syn*,s-*trans*-configuration. The orange, light-stable isomer, belongs to the monoclinic space group $P2_1/c$ and adopts an *anti*,s-*trans*-configuration. Raman and ^{13}C n.m.r. spectra for the orange isomer both in the solid state and in solution confirm that the solution species retains the structure established for the solid state. The Raman spectrum for the red isomer in the solid state shows the shift to lower wavenumber for the azo group stretching vibration characteristic of the *syn*,s-*trans*-configuration.

Photochromic materials are potentially useful for information storage and in various optical devices. The photochromism of inorganic compounds can be attributed to the formation of colour centres or to some other charge-transfer mechanism, whereas in organic and organometallic compounds photochromism usually involves a photoinduced isomerisation or dissociation which gives rise to differently coloured metastable species. There are advantages in using organometallic and organic photochromes in that their optical properties can be 'tuned' by making small structural adjustments, and they show greater changes in optical density than inorganic photochromes. However, they also show a greater tendency to fatigue on recycling. Consequently it is important to identify causes of fatigue in a photochromic system if that system is to be improved.

The formazans provide both organic and organometallic examples of photochromism;[1] the latter have been the more widely investigated. The Hg^{II} dithizone‡ complex is one of a small number of commercially exploited organic photochromes.

Apart from isomers which are unlikely because of serious steric crowding, the formazans can in principle adopt any of four possible structures (a)—(d) corresponding to *syn–anti* isomerisation about the C=N double bond and isomerisation about the C–N single bond (s-*cis*/s-*trans*). Otting and Neugebauer[2,3] have concluded that in solution the red and yellow formazans are, respectively, *syn*,s-*cis*- and *anti*,s-*trans*-isomers. In the solid state the formazans crystallise as red or orange-yellow solids, with the *syn*,s-*cis*[4] or *syn*,s-*trans*[5,6] configuration if red and the *anti*,s-*trans*[7–10] configuration if orange-yellow. However, no single photochromic formazan has yet been reported where both the red and the orange-yellow isomers have been obtained in the solid state and their structures established. Consequently, attempts to correlate photochromic behaviour with the nature of the substituents on C(1), C(3), and C(5) suffer from the absence of definitive structural information for both red and yellow isomers of a single photochromic formazan.

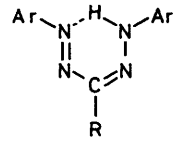

(a) *syn*,s-*cis*

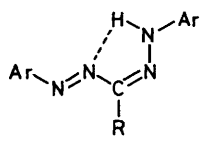

(b) *syn*,s-*trans*

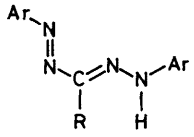

(c) *anti*,s-*cis*

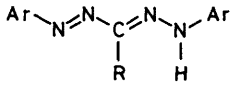

(d) *anti*,s-*trans*

We have been able to isolate the orange and the red conformers of 3-ethyl-1,5-diphenylformazan and now describe their *X*-ray crystal structures together with the results of i.r., Raman, and n.m.r. spectroscopic studies.

Experimental

Orange 3-Ethyl-1,5-diphenylformazan (**1**).—This was prepared by the method of Todd[11] and crystallised from 1:1 ethanol–water as orange *needles*, m.p. 96—98 °C (Found: C, 71.1; H, 6.5; N, 22.5. $C_{15}H_{16}N_4$ requires C, 71.4; H, 6.4; N, 22.2%).

Crystal structure analysis. An irregularly shaped crystal of dimensions 0.30 × 0.15 × 0.075 mm was used. Intensity data were collected at −150 °C with a Nicolet R3m four-circle diffractometer using graphite-monochromated Mo-K_α radiation. The unit-cell parameters (Table 1) were determined by least-squares refinement of 25 accurately centred reflections ($24 < 2\theta < 26°$); 2 020 reflections were collected using the θ—2θ scan technique ($3 < 2\theta < 50°$) and variable scan rate (4.88—58.6° min^{-1}). Crystal stability was monitored by recording three standard reflections every 100 reflections; no significant variation was observed. Data reduction gave 1 800 unique reflections of which 1 372 had $I > 3[\sigma(I)]$ and these

† *Supplementary data* (see section 5.6.3 of Instructions for Authors, in the January issue). Full lists of bond lengths and angles, H-atom coordinates, and thermal parameters have been deposited at the Cambridge Crystallographic Data Centre.

‡ Bis-(1,5-diphenylthiocarbazonato-*N*,*S*-)mercury(II).

Table 1. Crystal data for 3-ethyl-1,5-diphenylformazan isomers

	Orange (**1**)	Red (**2**)
Formula	$C_{15}H_{16}N_4$	$C_{15}H_{16}N_4$
M	392.4	392.4
Crystal system	Monoclinic	Orthorhombic
a/Å	9.281(1)	5.211(11)
b/Å	17.986(2)	9.835(12)
c/Å	8.474(1)	25.950(60)
α/°	90	90
β/°	104.07(1)	90
γ/°	90	90
V/Å^3	1 373.2(3)	1 329.9(4)
F(000)	535.86	535.86
μ(Mo-K_α)/cm^{-1}	0.71	0.73
λ(Mo-K_α)/Å	0.710 69	0.710 69
D_c/g cm^{-3}	1.21	1.25
Z	4	4
Obs. refl.	1 372	515
R/R_w	0.0486/0.0625	0.059/0.067
Space group	$P2_1/c$	$P2_12_12_1$

Table 2. Atomic co-ordinates (× 10^4) and temperature factors (Å^2 × 10^3) for the orange isomer (**1**)

Atom	x	y	z	U^a
C(1)	6 722(2)	2 801(1)	2 063(3)	36(1)
C(2)	5 707(2)	2 171(1)	2 333(2)	26(1)
C(3)	4 570(2)	1 995(1)	798(2)	23(1)
N(1)	2 914(2)	2 858(1)	1 168(2)	26(1)
N(2)	3 307(2)	2 329(1)	246(2)	24(1)
N(3)	4 799(2)	1 450(1)	−299(2)	23(1)
N(4)	5 999(2)	1 090(1)	200(2)	25(1)
C(11)	6 214(2)	505(1)	−848(2)	25(1)
C(12)	5 161(2)	267(1)	−2 222(2)	29(1)
C(13)	5 493(3)	−331(1)	−3 098(3)	35(1)
C(14)	6 844(3)	−683(1)	−2 641(3)	40(1)
C(15)	7 889(3)	−455(1)	−1 271(3)	40(1)
C(16)	7 568(2)	137(1)	−369(3)	32(1)
C(21)	1 559(2)	3 231(1)	632(2)	25(1)
C(22)	674(2)	3 139(1)	−937(2)	29(1)
C(23)	−603(2)	3 558(1)	−1 431(3)	36(1)
C(24)	−1 024(2)	4 053(1)	−387(3)	44(1)
C(25)	−161(2)	4 129(1)	1 186(3)	43(1)
C(26)	1 131(2)	3 721(1)	1 696(3)	32(1)

[a] Equivalent isotropic U defined as one third of the trace of the orthogonalised U_{ij} tensor.

were used for the structure determination. Intensities were corrected for Lorentz-polarisation effects but no absorption correction was applied (μ = 0.71 cm^{-1}). Systematic absences uniquely specified the space group as $P2_1/c$.

The structure was solved by direct methods using the program SOLV,[12] which revealed the positions of all the non-hydrogen atoms. Isotropic refinement using blocked cascade least-squares methods converged at $R = 0.109$. The non-hydrogen atoms were then refined anisotropically. Hydrogen atoms were included at calculated positions except H(1), which was located from a difference map. They were refined by using the riding model with thermal parameters of 1.2U of their carrier atoms [d(C–N,C–H) = 0.96 Å]. The structure converged with $R = 0.0486$ and $R_w = 0.0625$. The function minimised was $\Sigma w(|F_o| - |F_c|)^2$, where $w = [\sigma^2(F_o) + 0.0009\,4F_o^2]^{-1}$; a final difference map showed no peaks greater than 0.25 e Å^3.

Red 3-Ethyl-1,5-diphenylformazan (**2**).—Crystals were grown by dissolving pure orange (**1**) (1 g) in light petroleum (500 cm^3; b.p. 40—60 °C) and allowing the solution to equilibrate in the dark. The volume was reduced to *ca.* 200 cm^3 using a vacuum oven; after 3 days at 0 °C the resulting solution had deposited red needles in low yield; m.p. 73—74 °C.

Table 3. Atomic co-ordinates (× 10^4) and temperature factors (Å^2 × 10^3) for the red isomer (**2**)

Atom	x	y	z	U
C(1)	4 432(21)	3 620(10)	689(4)	32(3)
C(2)	6 780(22)	2 715(11)	660(4)	31(3)
C(3)	6 780(24)	1 709(12)	1 102(5)	26(3)
N(1)	5 519(17)	903(9)	1 869(4)	26(3)[a]
N(2)	5 337(18)	1 804(8)	1 473(4)	21(3)[a]
N(3)	8 837(18)	688(9)	1 126(4)	21(3)[a]
N(4)	10 252(17)	646(9)	731(4)	23(3)[a]
C(11)	3 704(22)	914(11)	2 261(4)	22(3)
C(12)	3 962(22)	−91(11)	2 648(4)	24(3)
C(13)	2 233(24)	−128(11)	3 058(4)	28(3)
C(14)	220(24)	805(11)	3 092(4)	31(3)
C(15)	13(23)	1 767(12)	2 701(4)	31(3)
C(16)	1 694(19)	1 830(11)	2 290(4)	18(3)
C(21)	12 161(23)	−378(11)	755(4)	24(3)
C(22)	12 555(23)	−1 253(10)	1 159(5)	27(3)
C(23)	14 534(25)	−2 237(11)	1 147(4)	36(4)
C(24)	16 028(22)	−2 330(12)	726(4)	28(3)
C(25)	15 626(23)	−1 465(10)	390(4)	30(3)
C(26)	13 714(22)	−493(11)	325(4)	27(3)

[a] Equivalent isotropic U defined as one third of the trace of the orthogonalised U_{ij} tensor.

Crystal structure analysis. A small crystal (0.86 × 0.13 × 0.063 mm) of high mosaicity was used. Intensity data were collected at −150 °C with a Nicolet R3m four-circle diffractometer. The unit-cell parameters (Table 1) were determined by least-squares refinement of 18 accurately centred reflections with 14 < 2θ < 19°; 1 122 reflections were collected using the θ—2θ scan technique (3 < 2θ < 45°) and variable scan rate (4.0—29.3° min^{-1}). Crystal stability was monitored by recording three standard reflections every 100 measurements and no significant variation was observed. Data reduction gave 1 062 unique reflections of which 515 having $I > 3[\sigma(I)]$ were used in the subsequent structure analysis. The intensities were corrected for Lorentz-polarisation effects but no absorption correction was applied (μ = 0.73 cm^{-1}). Systematic absences uniquely specified the space group as $P2_12_12_1$.

The structure was solved by direct methods using the program RANT which revealed the positions of all the non-hydrogen atoms. Isotropic refinement converged with $R = 0.089$. Hydrogen atoms were inserted at calculated positions on appropriate carbon atoms, using the riding model with thermal parameters equal to 1.2U of their carrier atoms [d(CH) = 0.96 Å]. The position of H(1), bound to N(1), was located from a difference map and not further refined. The four nitrogen atoms were refined anisotropically and the structure converged with $R = 0.059$, $R_w = 0.067$. The function minimised was $\Sigma w(|F_o| - |F_c|)^2$ where $w = [\sigma^2(F_o) + 0.0005\,7F_o^2]^{-1}$; a final difference map showed no features greater than 0.3 e Å^3. All the programs used for data reduction and structure solution are included in the SHELXTL (Version 4.0)[12] package.

General Methods.—Raman spectra were recorded with a Spex 1401 spectrometer equipped with a Thorn EM1 6256 photomultiplier tube used in the photon counting mode. A Spectra Physics 164-01 Krypton ion laser was used as the Raman scattering source, operating at 647 and 676 nm. Band wavenumbers were calibrated by using the emission spectrum of neon, and typical slit widths of 200 μm were employed, giving a

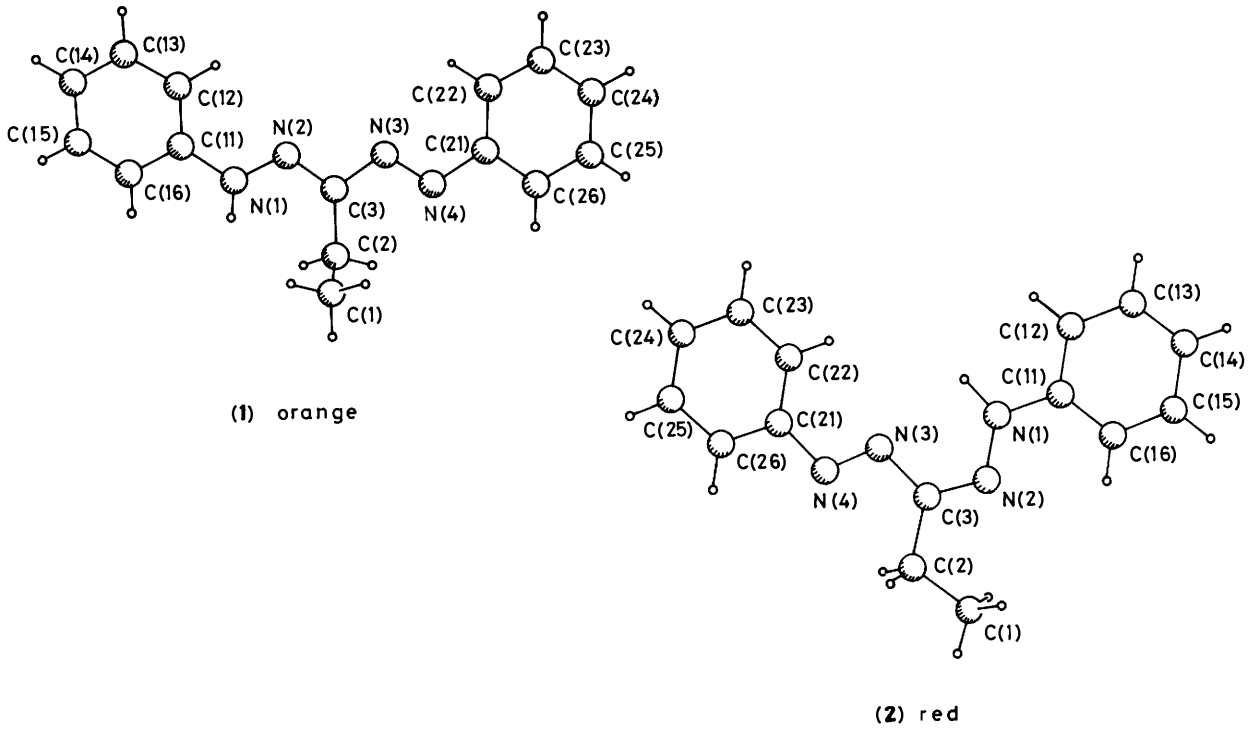

Figure 1. Molecular structures and atomic nomenclature of orange (**1**) and red (**2**) 3-ethyl-1,5-diphenylformazan

Table 4. A comparison of bond lengths and bond angles for the -N=N-C=N-N- backbone of the orange (**1**) and red (**2**) isomers

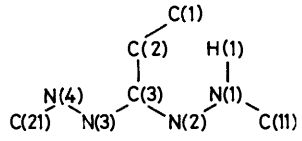

Bond lengths (Å)	Orange (**1**)	Red (**2**)
C(1)–C(2)	1.525(3)	1.515(16)
C(2)–C(3)	1.496(2)	1.520(17)
C(3)–N(2)	1.298(2)	1.308(15)
C(3)–N(3)	1.403(2)	1.379(15)
N(1)–N(2)	1.337(2)	1.361(13)
N(1)–C(11)	1.400(2)	1.389(15)
N(3)–N(4)	1.269(2)	1.265(13)
N(4)–C(21)	1.422(3)	1.417(15)
Bond angles (°)		
C(1)C(2)C(3)	111.0(2)	114.4(10)
C(2)C(3)N(2)	126.8(2)	116.8(10)
C(2)C(3)N(3)	122.4(2)	124.5(10)
N(2)C(3)N(3)	110.7(1)	118.6(10)
N(2)N(1)C(11)	120.2(1)	120.0(9)
C(3)N(2)N(1)	118.0(1)	117.5(9)
C(3)N(3)N(4)	113.5(1)	112.6(9)
N(3)N(4)C(21)	114.5(1)	113.3(9)
N(4)C(21)C(22)	124.9(2)	125.9(10)
N(4)C(21)C(26)	115.1(2)	115.6(10)
N(1)C(11)C(12)	121.9(2)	116.7(10)
N(1)C(11)C(16)	118.1(2)	124.1(10)

bandpass of 2 cm^{-1} at 647 nm. Samples were studied as crystals and as thin films sublimed onto glass substrates. Spectra were recorded at room temperature using laser powers of less than 50 mW so as to avoid sample decomposition.

I.r. spectra were recorded for KBr discs using a Bomem DA3 FTIR spectrometer.

Solid-state ^{13}C n.m.r. spectra were recorded at 50.3 MHz with a Varian Associates XL-200 spectrometer using a standard CP/MAS probe. Powdered samples (*ca.* 300 mg) were packed in rotors made of Kel-F and spun using MAS frequencies of 2—3 kHz. The combined techniques of high-power proton decoupling and single-contact cross polarisation (CP) were employed. Typical contact times of 50 ms were used, with recycle delays of 1.2 s. The number of transients acquired was of the order of 1 000.

Solution n.m.r. spectra were recorded at 20.00 MHz with a Varian Associates FT-80A spectrometer employing proton decoupling. In all cases either deuteriated solvents or a D_2O capillary insert provided the spin lock. Typical spectral parameters employed were: spectral width 5 000 Hz, acquisition time 1.023 s, pulse width 4 μs, number of transients 10 000—15 000. Quaternary carbon signals were identified by using pulse delays of up to 4 s. In some cases spin relaxation was assisted by the addition of chromium acetylacetonate to the spectroscopic solution. Samples of *ca.* 200 mg were used in 5 mm o.d. tubes with tetramethylsilane as internal standard.

Microanalyses were performed by Professor A. D. Campbell of the University of Otago.

Results and Discussion

Crystal Structures.—The molecular structures and atomic nomenclature for the orange (**1**) and red (**2**) isomers are shown in Figure 1. The final fractional atomic co-ordinates are given in Tables 2 and 3 and the bond lengths and angles for the -N–N=C–N=N- backbone are compared in Table 4. As found for all orange-yellow formazans in the solid state,[7–10] the orange isomer (**1**) adopts the *anti,s-trans* configuration whereas the red isomer (**2**) adopts the *syn,s-trans* configuration observed previously for the red crystals of 3-methylthio-1,5-diphenylformazan[5] and 3-carboxymethylthio-1,5-diphenylformazan.[6] No significant change is observed for the azo bond length in going from orange (**1**) to red (**2**) but there are significant changes in the remainder of the backbone. An increase in the mean C=N

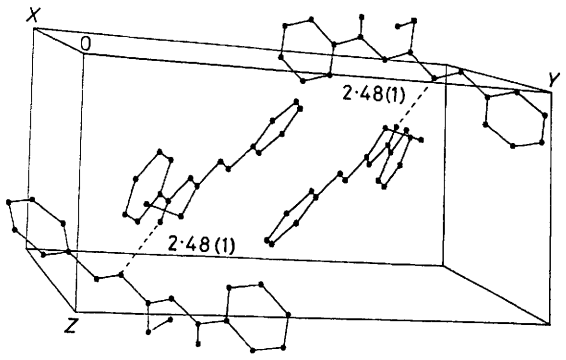

Figure 2. Unit-cell projection of orange (**1**) 3-ethyl-1,5-diphenylformazan. Bond length in Å

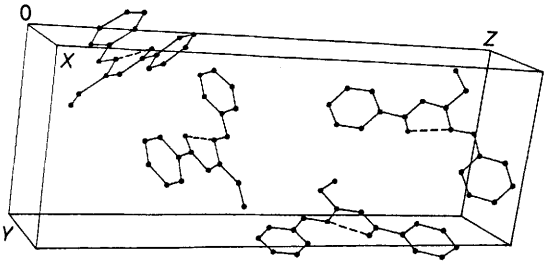

Figure 3. Unit-cell projection of red (**2**) 3-ethyl-1,5-diphenylformazan

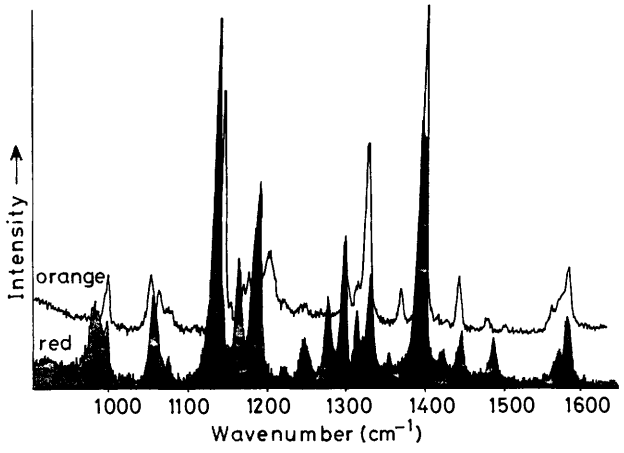

Figure 4. Raman spectra of orange (**1**) and red (**2**) 3-ethyl-1,5-diphenylformazan

bond length and an increase in the hydrazinyl N–N bond length accompany the orange *anti*,s-*trans* to red *syn*,s-*trans* change in configuration.

There is a rather long intermolecular hydrogen bond between H(1) and N(3) of adjacent molecules for orange (**1**) (see Figure 2) and a somewhat shorter intramolecular H(1) to N(3) bond length for red (**2**) (see Figure 3). The lower m.p. observed for red (**2**) is in accord with these observations.

The ethyl substituent on C(3) clearly represents a borderline functional group in that for formazans with small C(3) substituents such as –H, $-CH_3$, and =S, the orange *anti*,s-*trans* configuration is favoured whereas for formazans with the bulkier C(3) substituents, $-Bu^t$, $-NO_2$, –Ph, and –SMe either the *syn*,s-*trans* or the *syn*,s-*cis* configuration is thermodynamically more stable in the solid state at room temperature. It appears that the steric effect of the C(3) substituent is the most important factor in determining the configuration adopted by a particular formazan in the solid state. The electronic properties of the C(3) substituents and the effects of intra- or inter-molecular hydrogen bonding appear to play a secondary role.

Table 5. Raman bands (wavenumbers) observed for the orange (**1**) and red (**2**) isomers in the solid state

Orange (**1**)	Red (**2**)
1 603	1 600
1 591	1 590
1 583	
1 519	
1 500	1 504
1 461	1 461
1 411	1 408
1 372.5	
1 331.3	1 339
1 323.9	
1 306	1 306
	1 285
1 242	
1 208	
1 179	1 192
1 172	1 170
1 147	1 141
1 076	
1 059	1 062
1 051	
998.3	
993.8	

Raman Spectra.—Raman spectra for the light-stable structure (**1**) were obtained in solution and in the solid state, whereas for the dark-stable structure (**2**) the solution species was found to be unstable and only solid-state Raman data could be measured. Typical spectra for each structure are shown in Figure 4 with the band wavenumbers listed in Table 5.

The two most intense bands shift from 1 408 and 1 141 cm^{-1} in (**2**) to 1 411 and 1 147 cm^{-1} in (**1**). The bands at 1 408 and 1 411 cm^{-1} can be assigned to $\tilde{\nu}_{N=N}$ and the shift to higher wavenumber for the *anti*-s,*trans* structure parallels the change reported[13] for a Hg^{II} formazan complex. The bands at 1 141 and 1 147 cm^{-1} are assigned to a mode involving $\tilde{\nu}_{N-N}$. The substantial increase in the N–N bond order in (**1**) supports this assignment. Changes in the C–N bond order are reflected in the shift of the band at 1 339 cm^{-1} in (**2**) to bands at 1 372, 1 331, and 1 324 cm^{-1} in (**1**). The increase in the mean C–N bond order for (**2**) can account for the increase in wavenumber for the intense band at 1 331 cm^{-1} in the orange isomer (**1**) to 1 339 cm^{-1} in the red isomer (**2**). The increased bond order for the isolated C=N bond in the orange isomer (**1**) may explain the increased intensity for the band at 1 603 cm^{-1}. The other differences in the Raman spectra are the presence of bands at 1 242, 1 208, 1 076, and 1 051 cm^{-1} for (**1**) and a band at 1 285 cm^{-1} for (**2**).

I.r. Spectra.—The only difference detected in the i.r. absorption spectra of the red and orange isomers is the appearance of a weak band assigned as $\tilde{\nu}_{N-H}$ (see Figure 5) at 3 337 cm^{-1} for (**2**). Otherwise both structures appear to have identical i.r. spectra in the solid state, in contrast with the number of significant changes observed for their solid-state Raman spectra.

The appearance of a band at high wavenumber for the red isomer (**2**) parallels the earlier observation[14] of a band at 3 334 cm^{-1} for a fresh chloroform solution of 3-methylthio-1,5-diphenylformazan. Over a period of time in this solution the formation of the yellow isomer was observed, with the

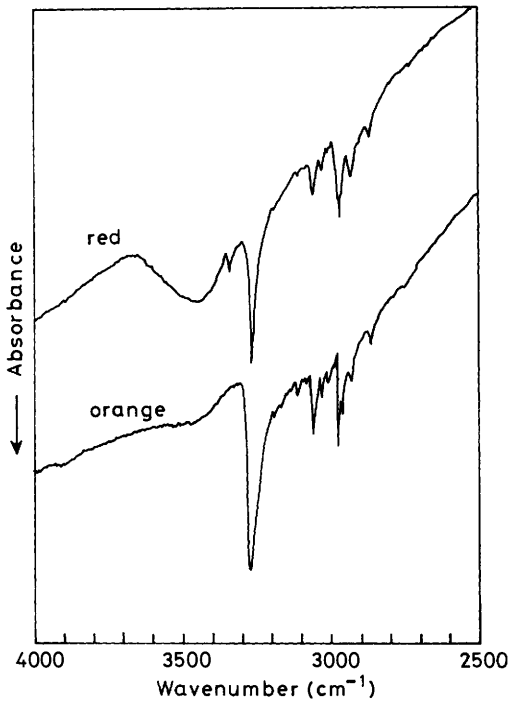

Figure 5. I.r. spectra of orange (**1**) and red (**2**) 3-ethyl-1,5-diphenylformazan

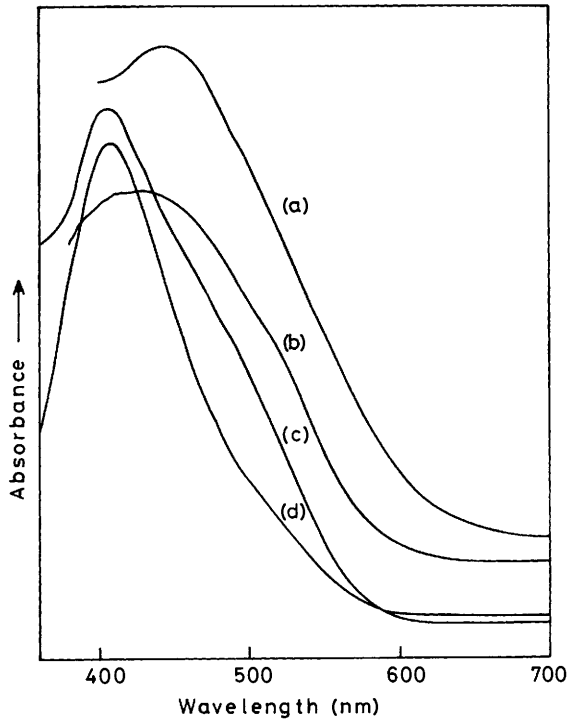

Figure 6. U.v.–Visible absorption spectra of 3-ethyl-1,5-diphenylformazan. Solvents (a) C_6D_6; (b) $CDCl_3$; (c) $(CD_3)_2CO$; (d) ethanol

Table 6. ^{13}C N.m.r. bands (p.p.m.) for the orange (**1**) and red (**2**) isomers in the solid state and in solution; relative intensities in parentheses

State	CH_2	CH_3	C(3)	C(11)	C(21)
Solid					
orange (**1**)	15.4	10.6	159.9	152.9	144.8
red (**2**)	22.5	10.1	153.3	149.2	144.2
Solution					
C_6D_6	23.7(15)	11.4(15)	156.0(3)	148.7(23)	149.9(11)
$CDCl_3$	23.3(17)	11.3(15)		148.5(14)	149.9(10)
			159.0(3)[a]		
	14.2(4)	9.5(4)		148.3(12)	
$(CD_3)_2CO$	23.3(11)	13.4(12)		149.4(14)	150.5(5)
			158.9(3)[a]		
	14.8(4)	9.5(3)		149.4(14)[b]	
EtOH	[Masked by solvent]			147.0(18)	
MeOH	18.4(11)	10.5(11)	157.0(2)	149.8(30)	

[a] Only one peak observed. [b] Peaks superimposed and assigned to both isomers.

appearance of a strong band at 3 240 cm^{-1}. This corresponds to the strong band observed at 3 268 cm^{-1} for the orange isomer (**1**).

^{13}C *N.m.r. Spectra.*—The ^{13}C n.m.r. resonances for the two isomers in the solid state are listed in Table 6. Assignments are based on the use of short contact times to identify quaternary carbon signals, TOSS experiments, and multiple spinner speeds to remove sidebands. Resonances for solution spectra are given for comparison.

In the solid spectra three signals for quaternary carbon are observed. The large shift in the C(3) signal in going from intramolecularly hydrogen bonded red (**2**) to intermolecularly bonded orange (**1**) reflects differences in the mean C=N bond order, $r_{C=N}$, with the greater electron density of (**2**) giving the expected lower-field resonance as compared with (**1**). A corresponding shift is noted for the ethyl resonances. Signals are observed for each of the quaternary aromatic carbon atoms C(21) and C(11). The differences are a reflection of the magnitude of shift expected for a carbon atom in proximity to an –N–H group. The C(11)–N–H resonances show a small conformation-dependent shift in going from (**2**) to (**1**) whereas the C(21)–N–H resonances are the same in both forms.

The ethyl group resonances provide a means of establishing the solvent dependence of the equilibrium between (**1**) and (**2**). The red isomer (**2**) is the dominant dark-stable species in C_6D_6, with the orange isomer becoming increasingly important as the solvent changes from $CDCl_3$ to hexadeuterioacetone and finally to ethanol. U.v. and visible absorption spectra measured on the actual samples used for the ^{13}C n.m.r. experiments (see Figure 6) confirm these conclusions. Data for the solution in hexadeuteriobenzene show that the red isomer is the major species, whereas in ethanol the orange isomer predominates.

In solution, rapid tautomerisation of the orange isomer (**1**) results in the collapse of the discrete signals for the aromatic quaternary carbon atoms into an averaged one. For the red isomer (**2**), the intramolecular hydrogen bond apparently inhibits such tautomerisation and signals for each of the aromatic quaternary carbon atoms are seen. When the two isomers are both present signals are observed for each isomer; $CDCl_3$ solutions yield three distinct signals for the quaternary aromatic carbon atoms of (**1**) and (**2**). The resonance for the third quaternary carbon atom, C(3), is more difficult to observe in solution; no evidence has been found for two distinct signals arising from the two isomers.

These same trends have been observed for all formazans of known crystal structure and will be outlined in a more comprehensive paper.[15]

Acknowledgements

One of the authors (C. W. C.) thanks the Maori Education Foundation for a Queen Elizabeth II Post-Graduate Scholarship.

References

1 G. H. Brown, 'Techniques of Chemistry, Vol. III, Photochromism,' Wiley-Interscience, New York, 1971.
2 W. Otting and F. A. Neugebauer, *Z. Naturforsch., Teil B*, 1968, **23**, 1064.
3 W. Otting and F. A. Neugebauer, *Chem. Ber.*, 1969, **102**, 2520.
4 E. Dijkstra, A. T. Hutton, H. M. N. H. Irving, and L. R. Nassimbeni, *Acta Crystallogr., Sect. B*, 1982, **38**, 535.
5 J. Preuss and A. Gieren, *Acta Crystallogr., Sect. B*, 1975, **31**, 1276.
6 A. T. Hutton, H. M. N. H. Irving, L. R. Nassimbeni, and G. Gafner, *Acta Crystallogr., Sect. B*, 1979, **35**, 1354.
7 Yu. A. Mel'chenko, Yu. D. Kondrashev, S. L. Ginzburg, and M. G. Neiganz, *Cristallografiya*, 1974, **19**, 522.
8 M. Laing, *J. Chem. Soc., Perkin Trans. 2*, 1977, 1248.
9 J. Guillerez, C. Pascard, and T. Prange, *J. Chem. Res.*, 1978, (*S*) 308; (*M*), 1978, 3934.
10 A. T. Hutton, H. M. N. H. Irving, and L. R. Nassimbeni, *Acta Crystallogr., Sect. B*, 1980, **36**, 2071.
11 D. Todd, 'Experimental Organic Chemistry,' Prentice-Hall Inc., New Jersey, 1979, p. 251.
12 G. M. Sheldrick, 'SHELXTL User Manual, Revision 4,' Nicolet XRD Corp., Madison, Wisconsin.
13 G. R. Burns and R. J. H. Clark, *Inorg. Chim. Acta*, 1984, **88**, 83.
14 G. R. Burns and J. F. Duncan, *Chem. Commun.*, 1966, 116.
15 C. Cunningham, G. R. Burns, and R. H. Newman, unpublished work.

Received 1*st October* 1987; *Paper* 7/1758